PHYSICAL REVIEW B, VOLUME 63, 201305(R)

Molecular-hydrogen interaction with β-SiC(100)3×2 and $c(4\times2)$ surfaces and with Si atomic lines

V. Derycke, P. Fonteneau,* N. P. Pham, and P. Soukiassian
Commissariat à l'Energie Atomique, DSM-DRECAM-SPCSI-SIMA, Bâtiment 462, Saclay, 91191 Gif sur Yvette Cedex, France and Département de Physique, Université de Paris-Sud, 91405 Orsay Cedex, France

(Received 29 January 2001; published 2 May 2001)

We investigate molecular H_2 interaction with β-SiC(100)3×2 and β-SiC(100) $c(4\times2)$ surfaces and with Si atomic lines by atom-resolved scanning tunneling microscopy and ultraviolet photoemission spectroscopy. While the 3×2 surface reconstruction remains totally inert, the $c(4\times2)$ is highly reactive to H_2 with sticking probabilities up to eight orders of magnitude higher than for Si(100)2×1. H_2 is initially dissociated at up-dimer adsorption sites influencing the two neighbor down dimers. At higher exposures, hydrogen induces a 2×1 surface transformation. This very high reactivity difference between 3×2 and $c(4\times2)$ reconstructions allows nonreacted Si atomic lines formation on a hydrogenated surface.

DOI: 10.1103/PhysRevB.63.201305 PACS number(s): 68.37.Ef, 68.35.−p, 82.65.+r

Silicon carbide (SiC) is an important semiconducting material having many potential applications.[1] From a fundamental aspect, it is a IV-IV compound semiconductor which, unlike covalent group-IV silicon or germanium has a significant charge transfer between C and Si atoms.[1–3] However, due to large differences in lattice parameters between cubic β-SiC and Si (−20%), and diamond (+22%), its (100) surface is very different from corresponding Si or Ge surfaces, with up to nine different reconstructions ranging from Si-rich to C-rich surfaces.[3–10] The surface terminated by one Si monolayer forms a $c(4\times2)$ reconstruction composed of alternately up and down dimers (AUDD) forming vertically undulated dimer rows.[3–5] This AUDD model has been established on the basis of scanning tunneling microscopy (STM) identifying the up and down dimers[5] and core-level photoemission using synchrotron radiation[6] experimental studies, and *ab initio* theoretical calculations.[7,8] The Si-rich surface is formed of dimer (asymmetric) rows in a 3×2 array. At the transition between 3×2 and $c(4\times2)$ reconstructions, selective Si atom thermal removal results in the self-organized formation of Si atomic lines.[9,10] These lines can form superlattices of massively parallel atomic lines (8×2, 5×2, 7×2, . . . surface reconstructions) or more separated lines including single isolated lines on top of the $c(4\times2)$ surface reconstruction. They are composed of Si dimers perpendicular to the atomic line direction.[9,10]

Semiconductor surface hydrogenation is important for both fundamental and technological reasons.[11,12] Hydrogen is a model system for surface reactivity. It is the most simple molecule having a well-known electronic structure. Its interaction with semiconductors can induce important surface structure or electronic transformations. Despite many experimental and theoretical studies, the hydrogenation of semiconductor surfaces is far from being fully understood. Surface passivation is also a field where hydrogen can play an important role. When possible, a fully hydrogenated surface is a good way to produce chemically inert surfaces.[12] Moreover, by nanometric or atomic scale transformation of a hydrogenated surface, it is possible to fabricate nanostructures in particular using STM.[13] Atomic lithography could then be performed by local surface dehydrogenation followed, e.g., by local oxidation of the nonpassivated area which is now routinely achieved for Si surfaces. Molecular H_2 is very reactive with metal surfaces such as transition metals. In contrast, semiconductor surfaces are inert to molecular hydrogen at room temperature and it is necessary to dissociate H_2 to obtain H-surface interaction. So far, there are two studies on atomic H/β-SiC only[14,15] with no such studies for molecular H_2.

In this Rapid Communication, we use STM and ultraviolet photoemission spectroscopy (UPS) to investigate room-temperature molecular H_2 interaction with β-SiC(100)3×2 and $c(4\times2)$ surface reconstructions. While the Si-rich 3×2 surface is totally inert to H_2, the Si-terminated $c(4\times2)$ reconstruction is strikingly found to be highly reactive (with sticking probabilities up to eight orders of magnitude larger than for Si), even at very low H_2 exposures, with H_2 dissociation and subsequent $c(4\times2)$ to 2×1 transition. H induces charge redistribution leading to a transition from an AUDD $c(4\times2)$ array to a structure where all dimers have the same height explaining the 2×1 surface ordering. Most interestingly, self-organized Si atomic lines on this Si-terminated surface remain totally unaffected by H, even when the surface is totally covered.

The STM experiments are performed at pressures $<8\times10^{-11}$ Torr. Our STM topographs are reproducible and not tip dependent. UPS data are collected at a base pressure $<4\times10^{-11}$ Torr using the Ne I line ($h\nu=16.85$ eV) and a hemispherical electrostatic electron analyzer. Thoroughly baked gas lines bring research grade molecular hydrogen into the chamber. STM topographs were acquired during H_2 exposures with turned off gauges to avoid atomic H formation. The tunneling current do not induce H_2 dissociation since the STM topographs of scanned surface areas look the same after H_2 exposures than the nonscanned ones. All other experimental details in particular, about high-quality β-SiC(100) surface preparation can be found elsewhere.[3–6,9,10]

We first look at the effect of H_2 on the Si-rich 3×2 and Si-terminated $c(4\times2)$ β-SiC(100) surface reconstructions

 ©2001 The American Physical Society

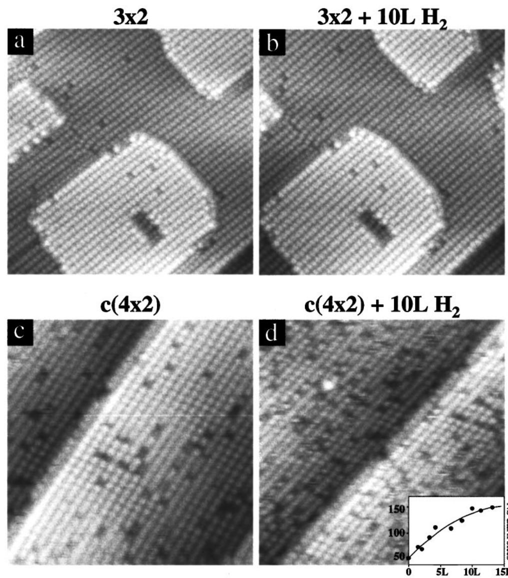

FIG. 1. (a) and (b) H_2/β-SiC(100)3×2: 300 Å×300 Å STM topographs (filled states) of clean (a) and 10 L exposed surface (b). (c) and (d) H_2/β-SiC(100)$c(4\times2)$: 200 Å×200 Å STM topographs (filled states) of clean (c) and 10 L H_2 exposed surface (d). The number of H adsorption sites versus H_2 exposures is also displayed in (d). The tip bias is $V_t=-3$ V at a 0.2 nA tunneling current.

using STM. Figure 1 displays STM topographs for clean and 10 H_2 L, where $1\,L=10^{-6}$ Torr s exposed 3×2 and $c(4\times2)$ surfaces. On the clean $c(4\times2)$ surface, we observe spot rows with each spot corresponding to the up Si dimers of the AUDD model.[5] Note that the first image has been recorded before total attenuation of the piezo drift in order to minimize the possible contamination of this highly sensitive $c(4\times2)$ surface during stabilization. A small residual drift distorts the usual pseudohexagonal arrangement of the dimers on image 1c, but this effect disappears later [Fig. 1(d)] and the usual characteristic $c(4\times2)$ pattern is seen.[5] One can clearly see that, while the β-SiC(100)3×2 exhibits no change upon H_2 exposure, the β-SiC(100) $c(4\times2)$ surface is significantly affected by new dark spots indicating hydrogen interaction with up dimers. Such a reaction implies H_2 molecule dissociation. Figure 1(d) inset displays a plot representing the number of dark sites versus H_2 exposures. From the initial slope, one can derive the room-temperature molecular hydrogen sticking probability on the β-SiC(100) $c(4\times2)$ surface at $s_0=2\times10^{-3}$. Interestingly, this value is very high, especially when compared to the Si(100) surface where H_2 sticking probabilities are $s_0<1\times10^{-11}$ for terraces and $s_0<1\times10^{-4}$ at step edges.[16]

Complementary atomic scale information about H_2 interaction on the β-SiC(100) $c(4\times2)$ surface reconstruction could be found by looking at empty electronic states topographs (Fig. 2). Each spot now corresponds to a down Si-dimer in agreement with the AUDD model.[5,7,8] Figure 2(a)–2(c) show the clean surface, and the same area after 1.4 L and 2.5 L H_2 exposures. It is clear that each event now appears as two dark spots instead of a single one as observed above in the filled states. This very interesting behavior indicates that, while the H atoms interact with up-dimers, it affects significantly the two down-dimer nearest neighbors belonging to the same row.

Additional insights about the H interaction process with the β-SiC(100) surfaces could be found by looking at the corresponding valence band (VB) obtained by UPS. Figures 3(a) and 3(b) display representative VB spectra for clean and H_2 covered 3×2 (a) and $c(4\times2)$ (b) surfaces. Both clean surfaces exhibit bulk (B) and surface (S_a and S_b) electronic states, the latter related to Si dimers and located in the band gap.[17,18] The β-SiC(100)3×2 VB spectra show no change with H_2 exposures further stressing that the surface is not reacting to H in excellent agreement with the above real-space STM surface imaging. Instead, the $c(4\times2)$ surface state S_b is rapidly quenched upon H_2 exposures indicating a strong interaction with the Si dimers, very likely through the dangling bonds. Since STM involves tunneling from the surface states, this behavior explains why reacted H sites appears dark in the STM filled state topographs (Fig. 1). No more VB change occurs at higher H_2 exposures indicating saturation while the VB still has significant density of states below E_F, with a surface exhibiting a 2×1 low-energy electron diffraction diagram.

Our above results indicate that a H_2 molecule reacts with an up-dimer of the β-SiC(100) $c(4\times2)$ surface reconstruction with subsequent dissociation and H atom adsorption on dangling bonds producing a double hydrogenated dimer (monohydride). This behavior is very different for the Si(100)2×1 surface on which H_2 dissociation takes place at

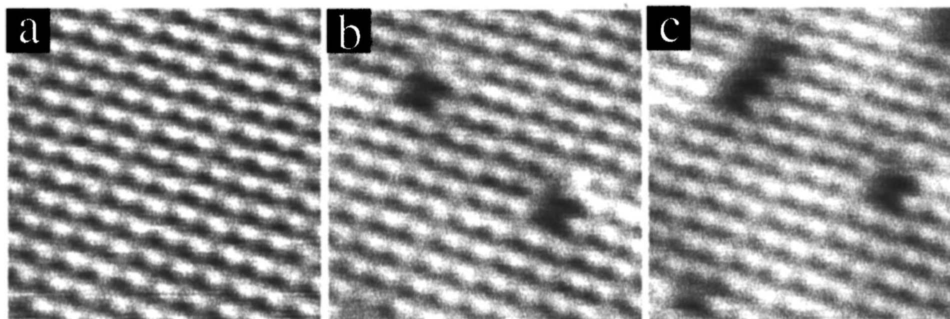

FIG. 2. β-SiC(100) $c(4\times2)$ surface 75 Å×75 Å STM topographs (empty states) for (a) clean, (b) 1.4 L, and (c) 2.5 L of H_2 exposed surfaces. The tip bias is $V_t=+3$ V at a 0.2 nA tunneling current.

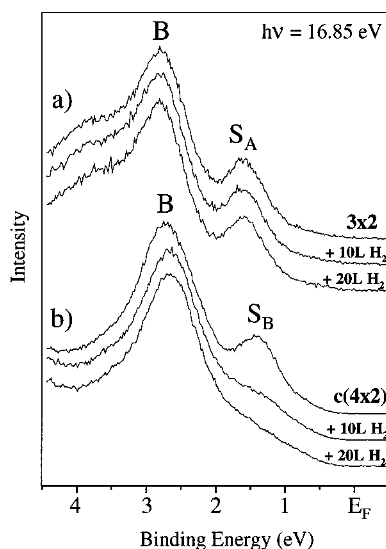

FIG. 3. Valence-band photoemission spectra ($h\nu = 16.85$ eV) for clean and H_2 exposed to 10 L and 20 L of (a) β-SiC(100)3 ×2 and (b) β-SiC(100) $c(4\times2)$ surfaces.

steps or defects only, the terraces remaining inert at room temperature (sticking coefficient $s_0 < 10^{-11}$).[16] This very different situation between β-SiC(100) and Si(100)2×1 surfaces results from major electronic and structural differences. Indeed, on the latter, lattice distortions, stressed backbond relaxation, and electronic redistribution around E_F play a crucial role in the process. The β-SiC(100) $c(4\times2)$ surface reconstruction has characteristics (structure, stress, and/or electronic properties) very different from those of Si(100)2 ×1, which might be at the origin of reactivity differences, including a very high sticking probability of $s_0 < 2\times10^{-3}$. Furthermore, the fact that a low-temperature annealing (700 °C) of the hydrogenated surface eliminates the dark reacted spots observed in the STM topographs and restores the $c(4\times2)$ surface reconstruction, indicates that these reacted dark sites do not correspond to missing dimers. This behavior also shows that the H interaction does not result in surface etching, with no thermal desorption of Si-H radicals upon annealing.

Another interesting aspect of H interaction with the $c(4\times2)$ surface could be found in looking at possible room-temperature H atom migration and/or hoping. In fact, such

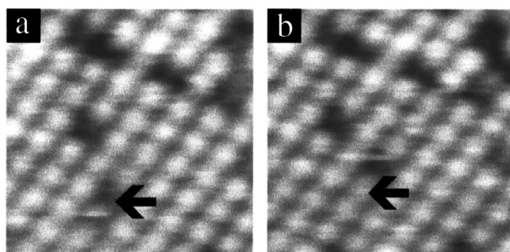

FIG. 4. 50 Å×50 Å STM topographs (filled states) showing the time dependence of H migration along a dimer row (arrow) on the β-SiC(100) $c(4\times2)$ surface at (a) $t=0$ and (b) $t=1$ minute later. The tip bias is $V_t = -3$ V at a 0.2 nA tunneling current.

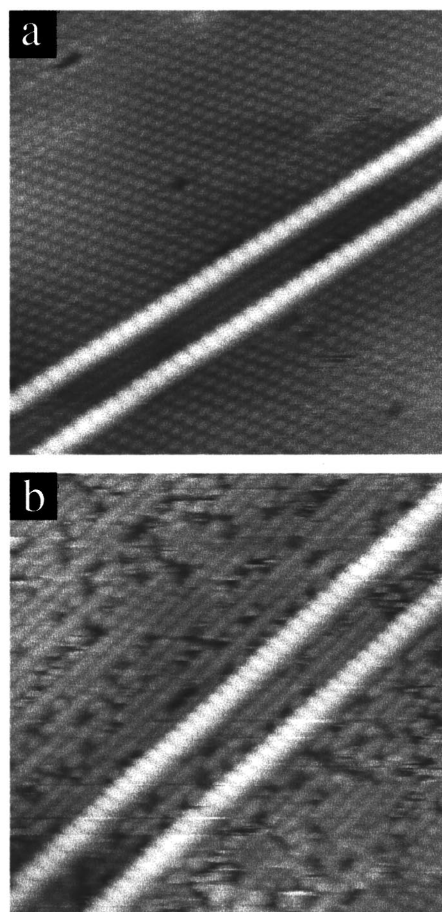

FIG. 5. 200 Å×200 Å STM topographs (filled states) showing the H influence on Si self-organized atomic lines built on a β-SiC(100) $c(4\times2)$ surface. One can notice that H reacts with the surface (becoming 2×1) and not with the Si atomic lines which remain unaffected.

mechanisms have been observed for Si(100)2×1 and Si(100)7×7 surfaces.[19] Figure 4 displays STM topographs for the same β-SiC(100) $c(4\times2)$ surface exposed to L of H_2 and recorded at 1 min interval time. One can clearly observed that the dark spot indicated by an arrow has moved along the dimer row. We repetitively observe such a behavior with no apparent hoping perpendicularly to the dimer rows.

We now turn to the $c(4\times2)$ to 2×1 symmetry change upon H_2 exposures. Notice that such a transition is reversible since thermal H desorption restores the original $c(4\times2)$ surface. Such a 2×1 transition results from the Si dimers (having an initial AUDD) coming at the same height upon H bonding to the Si dangling bonds. Indeed, such a mechanism is likely to induce sufficient charge redistribution probably leading to relief the surface stress at the origin of the $c(4\times2)$ AUDD array.[5] An apparent similar $c(4\times2)$ to 2×1 transition is indeed taking place at elevated temperature (400 °C) with all dimers also coming at the same height.[17] However, the temperature $c(4\times2)$ to 2×1 transition is definitively different from the hydrogen-induced one. The former, induced by temperature, results in a metallic 2×1

surface (as evidenced by scanning tunneling spectroscopy and by UPS),[17] while the 2×1 H-induced surface remains semiconducting as evident from the lack of density of states at the Fermi level [Fig. 3(b)].

Since the self-organized Si atomic lines are derived from the 3×2 surface dimer rows and are lying on the $c(4\times2)$ surface reconstruction, it is indeed challenging to also probe their reactivity to H_2. Figures 5(a) and 5(b) display 200 Å $\times$200 Å filled states STM topographs of two atomic lines for clean and 10 LH_2 exposed surfaces. One can see in Fig. 5(b) that, while the underlying $c(4\times2)$ surface turns to a dominant 2×1 array, none of these dimer lines are at all affected by hydrogen with no defect creation, further stressing the extremely high stability of these Si atomic lines. This also indicates that the portion of the surface located below an atomic line is not influenced by hydrogen. Finally, one should note that, in this way, we have Si dimer lines lying on a passivated surface having no more dangling bonds.

In conclusion, we investigate H_2 interaction with β-SiC(100)3×2 and $c(4\times2)$ surface reconstructions, and with Si atomic lines by STM and UPS. Unlike the totally inert 3×2 surface the $c(4\times2)$ reconstruction is highly reactive to H_2 with sticking probabilities up to eight orders of magnitude higher than for Si(100)2×1. H_2 is initially dissociated at up-dimer adsorption sites influencing the two neighbor down dimers. At higher exposures, hydrogen induces a 2×1 surface transformation. The important reactivity difference between 3×2 and $c(4\times2)$ surfaces allows nonreacted Si atomic lines formation on top of hydrogenated and passivated surface. This investigation opens up a wide range of possibilities to investigate reactions on β-SiC(100) surfaces and on atomic lines which exhibit very different reactivity depending on surface reconstruction and stoichiometry.

We wish to thank T. Billon, L. di Cioccio, and C. Pudda (CEA-LETI) for providing high-quality β-SiC(100) samples.

*Present address: STMicroelectronics, 38926 Crolles, France.

[1] *Silicon Carbide A Review of Fundamental Questions and Applications to Current Device Technology*, edited by W. J. Choyke, H. M. Matsunami, and G. Pensl (Akademie Verlag, Berlin, 1998), Vols. I & II, and references therein.

[2] V. M. Bermudez, Phys. Status Solidi B **202**, 447 (1997), and references therein.

[3] P. Soukiassian, Mater. Sci. Eng., B **61**, 506 (1999), and references therein.

[4] F. Semond, P. Soukiassian, A. Mayne, G. Dujardin, L. Douillard, and C. Jaussaud, Phys. Rev. Lett. **77**, 2013 (1996).

[5] P. Soukiassian, F. Semond, L. Douillard, A. Mayne, G. Dujardin, L. Pizzagalli, and C. Joachim, Phys. Rev. Lett. **78**, 907 (1997); V. Derycke, P. Fonteneau, and P. Soukiassian, Phys. Rev. B **62**, 12 660 (2000).

[6] V. Yu. Aristov, H. Enriquez, V. Derycke, P. Soukiassian, G. Le Lay, C. Grupp, and A. Taleb-Ibrahimi, Phys. Rev. B **60**, 16 553 (1999).

[7] A. Catellani, G. Galli, F. Gygi, and F. Pellacini, Phys. Rev. B **57**, 12 255 (1998).

[8] L. Douillard, F. Semond, V. Yu. Aristov, P. Soukiassian, B. Delley, A. Mayne, G. Dujardin, and E. Wimmer, Mater. Sci. Forum **264-268**, 379 (1998).

[9] P. Soukiassian, F. Semond, A. Mayne, and G. Dujardin, Phys. Rev. Lett. **79**, 2498 (1997).

[10] V. Derycke, N. P. Pham, P. Fonteneau, P. Soukiassian, P. Aboulet-Nze, Y. Monteil, A. J. Mayne, G. Dujardin, and J. Gautier, Appl. Surf. Sci. **162**, 413 (2000).

[11] K. Oura, V. G. Lifshits, A. A. Saranin, A. V. Zotov, and M. Katayama, Surf. Sci. Rep. **35**, 1 (1999).

[12] G. S. Higashi and Y. J. Chabal, in *Handbook of Silicon Wafer Cleaning Technology: Science, Technology and Applications*, edited by W. Kern (Noyes, Park Ridge, NJ, 1993), p. 433.

[13] E. T. Foley, A. F. Kam, J. W. Lyding, and Ph. Avouris, Phys. Rev. Lett. **80**, 1336 (1998).

[14] H. W. Yeom, I. Matsuda, Y. C. Chao, S. Hara, S. Yoshida, K. Kajimura, and R. I. G. Uhrberg, Phys. Rev. B **61**, R2417 (2000).

[15] B. I. Craig and P. V. Smith, Surf. Sci. **233**, 255 (1990); Physica B **170**, 518 (1991).

[16] P. Kratzer, E. Pehlke, M. Scheffler, M. B. Rascke, and U. Höfer, Phys. Rev. Lett. **81**, 5596 (1998), and references therein.

[17] V. Yu. Aristov, L. Douillard, O. Fauchoux, and P. Soukiassian, Phys. Rev. Lett. **79**, 3700 (1997).

[18] H. W. Yeom, Y. C. Chao, I. Matsuda, S. Hara, S. Yoshida, and R. I. G. Uhrberg, Phys. Rev. B **58**, 10 540 (1998).

[19] J. J. Boland, Phys. Rev. Lett. **65**, 3325 (1990); **67**, 1539 (1991); Surf. Sci. **261**, 17 (1992).